Accuracy Enhancement of Second-Order Cone Relaxation for AC Optimal Power Flow via Linear Mapping

Khalil Gholami[1], Ali Azizivahed[2], Li Li[2], Jiangfeng Zhang[3]

[1] Department of Electrical Engineering, Kermanshah Branch, Islamic Azad University, Kermanshah, Iran. (e-mail: kgholami212@gmail.com)

[2]Faculty of Engineering and Information Technology, University of Technology Sydney, Australia (e-mails: Ali.Azizivahed@student.uts.edu.au; li.li@uts.edu.au).

[3]Department of Automotive Engineering at Clemson University (e-mail: jiangfz@clemson.edu).

Abstract

Optimal power flow (OPF) has always been one of the most crucial tools for power system operations. OPF problem formulation involves non-linear alternative current (AC) power flow equations, and a wide range of challenges occur as a result. This is because the resulting non-convex optimization problems are not only complex and time-consuming, but also difficult to find a global optimum as many local optimums are present. So far, different relaxations have been provided to address these issues. One of the most effective strategies for convexifying such formulations is second-order cone programming (SOCP). Although SOCP is an efficient instrument for convexifying AC OPF equations, it is unable to reach the global optimal solution compared to other methods. The aim of this paper is therefore to provide a new method to approach the global optimum of AC OPF relaxed by SOCP. This method is obtained with the aid of a new linrear tranfsormation called semi-Lorentz transformation as it similar to the Lorentz transformation in the special relativity theory. In this method second-order cone AC OPF equations are mapped to a new model via semi-Lorentz transformation. In addition, an approximation approach is also presented to reach the best semi-Lorentz factor, the main driver in semi-Lorentz transformation, for each particular problem based on the network parameters. From the comparative analysis in case studies, the proposed OPF solution method has robust precision and higher efficiency while consuming less computing time.

Keywords: Optimal Power Flow, Second-Order Cone Programming, Linear mapping, Tightened Second-Order Cone Programming relaxation.

1. Introduction

Optimal power flow (OPF) is an important method to optimize power system operations. The objective of OPF is to minimize an objective function comprising generation cost, power loss, etc., subject to equality and inequality system constraints. Considering the non-linear and non-convex functions involved in the OPF formulation, this OPF is an NP-hard problem [1]. Thus it has attracted continuing research interest for decades in finding more effective solution methods. As an example of recent approaches to OPF, population-based algorithms were widely utilized to solve OPF. In this case, researchers in [2] got an invasive weed optimization algorithm improved by chaos to solve non-convex OPF. Modified imperialist competitive algorithm was also used to solve multi-objective OPF in [3]. Similarly, Ref. [4] presents a solution method on the basis of adaptive grasshopper optimization algorithm to solve the OPF problem. Although OPF can be solved in [2]–[4], it has a significant computational burden, and the global optimal result is not guaranteed [5], [6].

Despite the aforementioned techniques in [2]–[4], there are relaxation-based methods which can convert a non-convex OPF into a convex optimization problem to easily obtain the global optima while taking the advantages of powerful optimization solvers like CPLEX, and GUROBI.

There are several strategies associated with the aforementioned relaxation methods. Semi-definite programming (SDP) is one of the techniques that can be used in convexifying OPF [7], [8]. However, authors in [9] have identified its limitations in dealing with large-scale systems. Furthermore, SDP is quite time-consuming and merely presents accurate results for a few problems [10]–[12]. SDP is not an appropriate tool for OPF because it even failed to present accurate results for a two-node one-generator test network [13]. Another method for relaxation is quadratic convex programming (QCP) which has been utilized in some studies. For instance, Ref. [14] uses branch-and-cut algorithm to solve the OPF problem, where valid inequalities and bound tightening strategies [15] are incorporated

into the formulas. The mentioned valid inequalities are obtained on the basis of the convex hull definition of 2×2 rank-one positive semidefinite Hermitian matrices. Additionally, complex per unit normalization is presented for tightening QCP-based OPF in [16]. Despite the advantage of QCP in terms of large-scale problems, it requires more computation time and may not be suitable for real-time operations [17]. Second-order cone programming (SOCP) is a more promising technique for OPF. For example, the cutting plane method is employed to enhance the strength of SOCP to cope with OPF problems [18]. It has been found that QCP has provided better results in some cases compared to SOCP [19], but it is not computation-friendly.

According to the aforementioned review, both QCP and SOCP are appropriate for relaxing OPF problems. The main difference between them is that QCP can approach the global optimum better while SOCP is easier to implement and can compute faster [18]. Some studies show that it is possible to improve the accuracy of SOCP to approach the global optimum while keeping its fast computing feature. For example, a relaxed SOCP-based AC OPF using power loss relaxation is introduced in [19] to improve accuracy, and a cutting plane alternative is integrated into SOCP to better approximate the global optimum of OPF [20].

Following the above ideas, this paper aims to improve the accuracy of SOCP by the linear mapping approach [21]. After evaluating various linear mappings including shear mapping, rotation mapping, etc., a new linear transformation called semi-Lorentz transformation, which is similar to the Lorentz transformation in the special relativity theory, is eventually selected due to its positive influence in this regard. It is notable that the optimization results for the mapped OPF problem are obtained based on all linear transformations (including; rotation, shear, squeeze, reflection, and scaling), among which semi-Lorentz transformation has a better effect on transforming OPF equations and expression, leading to a lower optimality gap. To be more specific, linear semi-Lorentz transformation is performed on the SOCP-AC OPF equations, which will reduce the gap to the global

minimum and thus increase the accuracy of SCOP.

The contributions of the proposed approach are as follows:

- Two different transformations based on semi-Lorentz mapping for SOCP-AC OPF are presented. In the first model (model-A), both network variables and parameters are transformed. It clearly shows that the semi-Lorentz transformation directly affects the convex SOC constraint and provides more space for transformed variables to assign values that are more close to the values in AC OPF. In the second model (model-B), the network information (power demands and line impedances) is changed after transformation, and it provides input data (changed network information) to estimate the best value for the semi-Lorentz factor (which plays the main role in the semi-Lorentz transformation) for each case to reach the minimum optimality gap.
- Three different equations for three operation conditions (such as typical, congested conditions and small-angle difference) are presented to estimate the semi-Lorentz factor accurately based on network information (power demands and line impedances). The Pearson correlation [22] is also used to verify that the best value of semi-Lorentz factor (M) obtained by estimation methods is close enough to the values obtained empirically.

The rest of this paper is organized as follows. Section 2 presents the non-linear mathematical equations of the OPF, convexifying and tightened OPF. Numerical results under different case studies are provided in Section 3. The conclusion and future works are given in Section 4.

2. Problem formulation

2.1. A brief review of non-linear AC OPF

A brief review of the non-linear polar AC OPF is described here before portraying the proposed SOCP-AC OPF model. Like all other optimization problems, it has an objective function (1a) which is subject to a set of equality and inequality constraints (1b)-(1l). The objective function (1a) minimizes the generation cost. Constraints (1b) and (1c) guarantee the active and reactive power

balance at each node, respectively. The active and reactive power flows between branches are shown in constraints (1d)-(1g), respectively. Constraints (1h) and (1i) represent the real and reactive power boundary of the generative units, respectively. Constraint (1j) maintains the system voltage between acceptable ranges. The apparent power of each branch is controlled by means of constraints (1k) and (1l). To further elaborate the model, the specifications used in (1a)-(1l) are seen in Fig. 1.

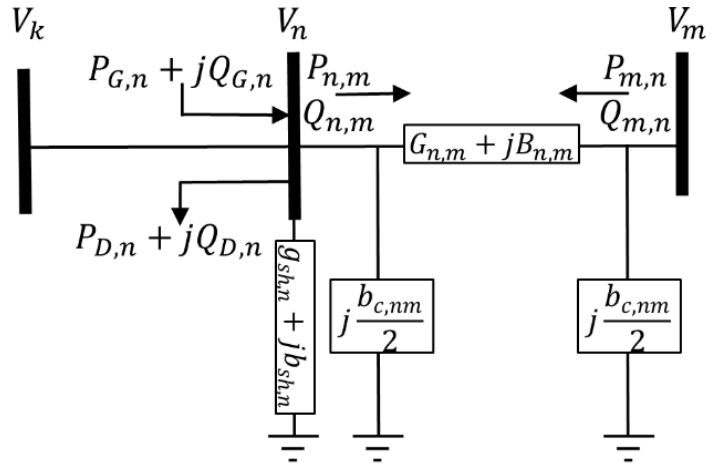

Fig. 1: Illustration of a transmission network

$$Min_{\forall t}[\mathcal{B}_{Cost}]$$

$$\mathcal{B}_{Cost} = \sum_{n\in\Omega_{bus}} \left(a_n P_{G,n}^2 + b_n P_{G,n} + c_n\right) \tag{1a}$$

$$s.t. \qquad \forall n, m \in \Omega_{bus} \ , \forall (n,m) \in \Omega_{brch}$$

$$P_{G,n} - P_{D,n} = g_{sh,n} V_n^2 + \sum_{\forall (n,m)\in\Omega_{brch}} P_{n,m} \tag{1b}$$

$$Q_{G,n} - Q_{D,n} = -b_{sh,n} V_n^2 + \sum_{\forall (n,m)\in\Omega_{brch}} Q_{n,m} \tag{1c}$$

$$P_{n,m} = G_{n,m}V_n^2 - G_{n,m}V_nV_m\cos\delta_{n,m} - B_{n,m}V_nV_m\sin\delta_{n,m} \tag{1d}$$

$$Q_{n,m} = -\left(B_{n,m} + \frac{b_{c,nm}}{2}\right)V_n^2 + B_{n,m}V_nV_m\cos\delta_{n,m} - G_{n,m}V_nV_m\sin\delta_{n,m} \tag{1e}$$

$$P_{m,n} = G_{n,m}V_m^2 - G_{n,m}V_nV_m\cos\delta_{n,m} + B_{n,m}V_nV_m\sin\delta_{n,m} \tag{1f}$$

$$Q_{m,n} = -\left(B_{n,m} + \frac{b_{c,nm}}{2}\right)V_m^2 + B_{n,m}V_nV_m\cos\delta_{n,m} + G_{n,m}V_nV_m\sin\delta_{n,m} \tag{1g}$$

$$P_{G,n}^{min} \le P_{G,n} \le P_{G,n}^{max} \tag{1h}$$

$$Q_{G,n}^{min} \le Q_{G,n} \le Q_{G,n}^{max} \tag{1i}$$

$$V^{min} \le V_n \le V^{max} \tag{1j}$$

$$P_{n,m}^2 + Q_{n,m}^2 \le \left(S_{n,m}^{max}\right)^2 \tag{1k}$$

$$P_{m,n}^2 + Q_{m,n}^2 \le \left(S_{n,m}^{max}\right)^2 \tag{1l}$$

In the above model, Ω_{bus} and Ω_{brch} are the set of nodes and branches, respectively; $P_{G,n}$ and $P_{D,n}$ represent the active generation and demand at node n, respectively; $Q_{G,n}$ and $Q_{D,n}$ denote the reactive generation and demand at node n; $G_{n,m}$ and $B_{n,m}$ are conductance and susceptance of the branch between nodes n and m, respectively; $b_{c,nm}$ is the shunt admittance of the branch between nodes n and m; $g_{sh,n}$ and $b_{sh,n}$ are shunt conductance and susceptance of node, respectively; $P_{n,m}$ and $Q_{n,m}$ are active and reactive power flows between nodes n and m, respectively; V_n represents the voltage at node n; $\delta_{n,m}$ is phase angle between nodes n and m; $P_{G,n}^{min}$ and $P_{G,n}^{max}$ are the active power lower and upper bounds of generation unit n, respectively; $Q_{G,n}^{min}$ and $Q_{G,n}^{max}$ show the reactive power bounds of generator n; V^{min} and V^{max} demonstrate the boundary of voltage magnitude; and $S_{n,m}^{max}$ is the maximum apparent power capacity of branch (n,m).

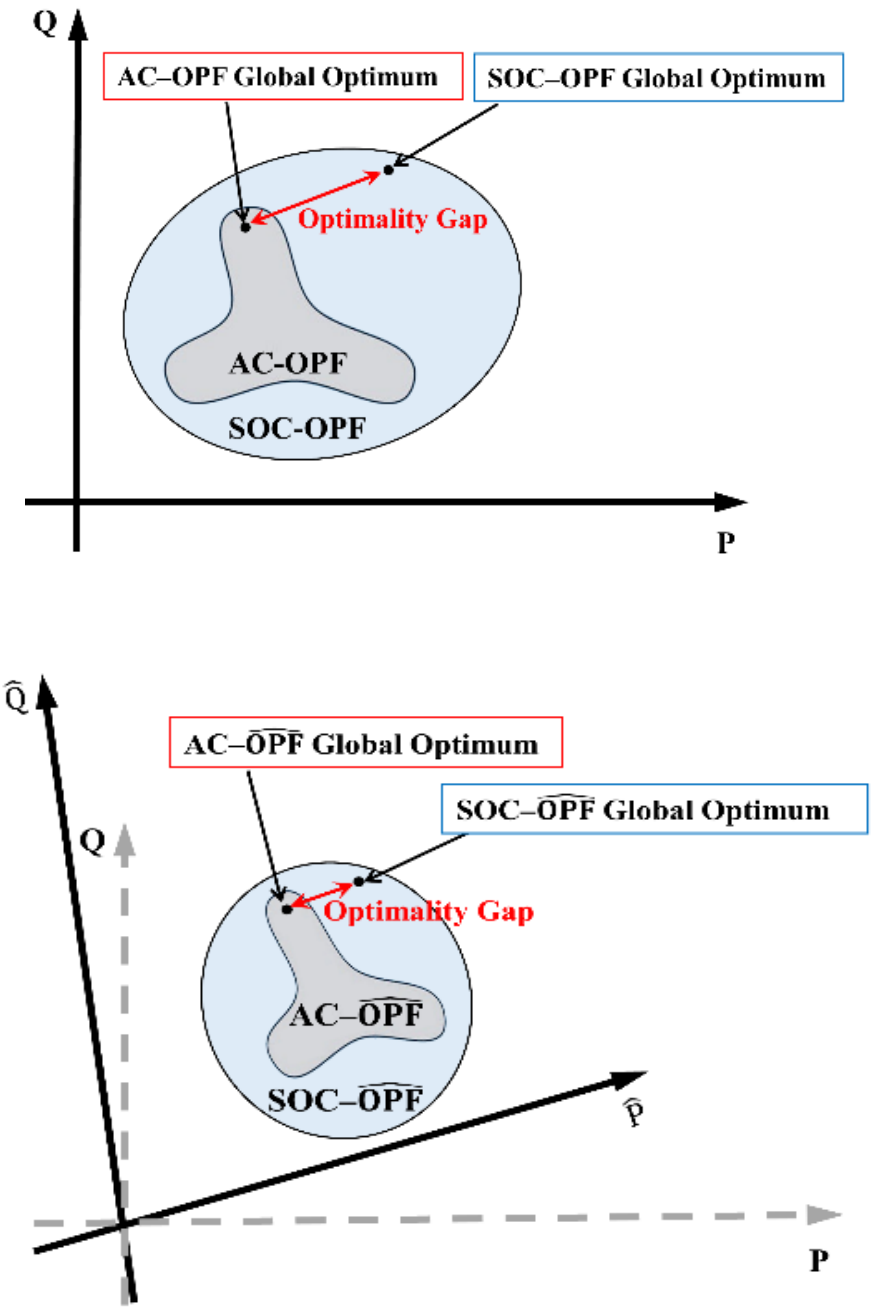

Fig. 2: SOCP relaxation of AC-OPF (upper), and transformation of SOCP-OPF and AC-OPF via linear mapping (Lower)

2.2. SOCP Relaxation of AC OPF

There are some non-linear terms in AC OPF equations in the previous section, such as V_n^2, $V_n V_m \cos\delta_{n,m}$, and $V_n V_m \sin\delta_{n,m}$. To linearize these non-linear terms, three new variables are introduced as follows;

$$\mathrm{K}_n = V_n^2 \quad ,\forall n \tag{2a}$$

$$\mathrm{T}_{n,m} = V_n V_m \cos\delta_{n,m} \quad ,\forall (n,m) \in \Omega_{brch} \tag{2b}$$

$$\mathrm{L}_{n,m} = V_n V_m \sin\delta_{n,m} \quad ,\forall (n,m) \in \Omega_{brch} \tag{2c}$$

$$\mathrm{T}_{n,m}^2 + \mathrm{L}_{n,m}^2 = \mathrm{K}_n \mathrm{K}_m \quad ,\forall (n,m) \in \Omega_{brch} \tag{2d}$$

where K_n, $\mathrm{T}_{n,m}$ and $\mathrm{L}_{n,m}$ are the newly introduced variables. The correlation between these three new variables is presented in (2d).

After defining the aforementioned variables, the technical constraints of the system are convexified and reformulated in the following manner:

$$Min_{\forall t}[\beta_{Cost}]$$

$$\beta_{Cost} = \sum_{n\in\Omega_{bus}} \left(a_n P_{G,n}^2 + b_n P_{G,n} + c_n\right) \tag{3a}$$

$$s.t. \qquad \forall n,m \in \Omega_{bus} \ ,\forall (n,m) \in \Omega_{brch}$$

$$P_{G,n} - P_{D,n} = g_{sh,n}\mathrm{K}_n + \sum_{\forall (n,m)\in\Omega_{brch}} P_{n,m} \tag{3b}$$

$$Q_{G,n} - Q_{D,n} = -b_{sh,n}\mathrm{K}_n + \sum_{\forall (n,m)\in\Omega_{brch}} Q_{n,m} \tag{3c}$$

$$P_{n,m} = G_{n,m}\mathrm{K}_n - G_{n,m}\mathrm{T}_{n,m} - B_{n,m}\mathrm{L}_{n,m} \tag{3d}$$

$$Q_{n,m} = -\left(B_{n,m} + \frac{b_{c,nm}}{2}\right)\mathrm{K}_n + B_{n,m}\mathrm{T}_{n,m} - G_{n,m}\mathrm{L}_{n,m} \tag{3e}$$

$$P_{m,n} = G_{n,m}\mathrm{K}_m - G_{n,m}\mathrm{T}_{n,m} + B_{n,m}\mathrm{L}_{n,m} \quad (3f)$$

$$Q_{m,n} = -\left(B_{n,m} + \frac{b_{c,nm}}{2}\right)\mathrm{K}_m + B_{n,m}\mathrm{T}_{n,m} + G_{n,m}\mathrm{L}_{n,m} \quad (3g)$$

$$P_{G,n}^{min} \le P_{G,n} \le P_{G,n}^{max} \quad (3h)$$

$$Q_{G,n}^{min} \le Q_{G,n} \le Q_{G,n}^{max} \quad (3i)$$

$$\left(V^{min}\right)^2 \le \mathrm{K}_n \le (V^{max})^2 \quad (3j)$$

$$P_{n,m}^2 + Q_{n,m}^2 \le \left(S_{n,m}^{max}\right)^2 \quad (3k)$$

$$P_{m,n}^2 + Q_{m,n}^2 \le \left(S_{n,m}^{max}\right)^2 \quad (3l)$$

$$\mathrm{T}_{n,m}^2 + \mathrm{L}_{n,m}^2 \le \mathrm{K}_n\mathrm{K}_m \quad (3m)$$

The equation (2d) related to the correlation between new variables is relaxed to (3m) for convexification. This convexification was presented in [22] for the first time.

This model now brings an opportunity to take advantage of commercial solvers. However, it is still not able to guarantee a solution that is close to the global optimum. Next section describes this problem, and then some alternative techniques are taken to tackle this inherited problem of relaxed AC OPF.

2.3. Implementing Linear Transformation on OPF Equations

Fig. 2 illustrates the optimality gap and the intent of this analysis, where optimality gap here means the difference between the best-known solution (as determined by AC OPF) and the best-found solution (the result of SOCP-AC OPF). This is an indicator for measuring the precision of relaxed methods [23]. Fig. 2 (upper) shows that the feasible domain of non-linear AC OPF is convexified to the feasible domain of the SOCP-OPF. As shown in Fig. 2 (lower), the hat ($\widehat{\ }$) sign is used to represent the mapped P-Q coordination and the mapped OPF problem under the linear mapping, and Fig.2 (upper) shows the original P-Q coordination and the original OPF problem. However, there is an optimality gap due to convexification. In other words, the optimal solution obtained by SOCP-

OPF is slightly different from the solution obtained by the AC OPF. To solve this problem, this paper will apply the linear semi-Lorentz transformation to the SOCP-OPF equations so that they are converted into new forms with smaller optimality gaps. The reason for applying linear transformation is to keep the feasible domain convex after transformation. Fig. 2 (lower) illustrates this idea, where the optimality gap turns smaller when the SOCP-OPF is transformed.

This linear transformation is defined by the following equations:

$$\begin{bmatrix}\hat{P}\\ \hat{Q}\end{bmatrix} = \gamma \begin{bmatrix}1 & -M\\ -M & 1\end{bmatrix}\begin{bmatrix}P\\ Q\end{bmatrix} \tag{4a}$$

$$\gamma = \frac{1}{\sqrt{1-M^2}} \tag{4b}$$

where, $-1 < M < 1$ is semi-Lorentz factor.

In the following, two different models are considered to apply the above linear transformation. In the first model, both variables and network parameters are mapped. Then according to the transformed version of the relaxed SOC constraint, it can be seen how the proposed linear transformation can reduce the relaxation error and consequently reduce the optimality gap (more details of the relaxation error and optimality gap are provided in Section 3.1). The question is: what is the best value of semi-Lorentz factor (*M*) to reach the minimum optimality gap for each system? The easiest way is to find it empirically and solve the transformed SOC-OPF for different values of *M*, which is very time-consuming. The other way is to estimate it based on the network information (known parameters such as power consumption and branch impedance). To this end, the second model is provided in which only the network parameters are changed based on the proposed linear transformation. The mapped parameters in this model are used to estimate the best value for *M* for each system separately.

2.3.1. Model-A: transforming both variables and network parameters

The target of transformation in this model is both variables and network parameters. The branch parameters (shunt and mutual impedances), the bus parameters (shunt impedance), and the variables

consisting of $\left(\mathrm{T}_{n,m}, \forall(n,m)\in\Omega_{brch}\right)$ & $\left(\mathrm{L}_{n,m}, \forall(n,m)\in\Omega_{brch}\right)$ are mapped. Then, the OPF equations are reformulated as follows when the variables are transformed.

$$Min_{\forall t}[\mathcal{B}_{Cost}]$$

$$\mathcal{B}_{Cost} = \sum_{n\in\Omega_{bus}} a_n\left(\gamma\left(\hat{P}_{G,n} + M\hat{Q}_{G,n}\right)\right)^2 + b_n\left(\gamma\left(\hat{P}_{G,n} + M\hat{Q}_{G,n}\right)\right) + c_n \tag{5a}$$

$$s.t. \qquad \forall n,m \in \Omega_{bus}\ , \forall(n,m) \in \Omega_{brch}$$

$$\begin{aligned}\hat{P}_{G,n} - \hat{P}_{D,n} &= \gamma\left(g_{sh,n} + Mb_{sh,n}\right)K_n + \sum_{\forall(n,m)\in\Omega_{brch}} \gamma\left(P_{n,m} - MQ_{n,m}\right) \\ &= \breve{g}_{sh,n}K_n + \sum_{\forall(n,m)\in\Omega_{brch}} \hat{P}_{n,m}\end{aligned} \tag{5b}$$

$$\begin{aligned}\hat{Q}_{G,n} - \hat{Q}_{D,n} &= -\gamma\left(b_{sh,n} + Mg_{sh,n}\right)K_n + \sum_{\forall(n,m)\in\Omega_{brch}} \gamma\left(Q_{n,m} - MP_{n,m}\right) \\ &= -\breve{b}_{sh,n}K_n + \sum_{\forall(n,m)\in\Omega_{brch}} \hat{Q}_{n,m}\end{aligned} \tag{5c}$$

$$\begin{aligned}\hat{P}_{n,m} = \gamma\Bigg(&\left(G_{n,m} + M\left(B_{n,m} + \frac{b_{c,nm}}{2}\right)\right)\mathrm{K}_n - G_{n,m}\left(\mathrm{T}_{n,m} - M\mathrm{L}_{n,m}\right) \\ &- B_{n,m}\left(\mathrm{L}_{n,m} + M\mathrm{T}_{n,m}\right)\Bigg) \\ = &\left(\breve{G}_{n,m} + \frac{\breve{g}_{c,nm}}{2}\right)\mathrm{K}_n - G_{n,m}\hat{T}_{n,m} - B_{n,m}\hat{L}_{n,m}\end{aligned} \tag{5d}$$

$$\begin{aligned}\hat{Q}_{n,m} = \gamma\Bigg(&-\left(B_{n,m} + \frac{b_{c,nm}}{2} + MG_{n,m}\right)\mathrm{K}_n + B_{n,m}\left(\mathrm{T}_{n,m} + M\mathrm{L}_{n,m}\right) \\ &- G_{n,m}\left(\mathrm{L}_{n,m} - M\mathrm{T}_{n,m}\right)\Bigg) \\ = &-\left(\breve{B}_{n,m} + \frac{\breve{b}_{c,nm}}{2}\right)\mathrm{K}_n + B_{n,m}\breve{T}_{n,m} - G_{n,m}\breve{L}_{n,m}\end{aligned} \tag{5e}$$

$$\hat{P}_{m,n} = \gamma\left(\left(G_{n,m} + M\left(B_{n,m} + \frac{b_{c,nm}}{2}\right)\right)\mathrm{K}_m - G_{n,m}\left(\mathrm{T}_{n,m} + M\mathrm{L}_{n,m}\right)\right.$$

$$\left. + B_{n,m}\left(\mathrm{L}_{n,m} - M\mathrm{T}_{n,m}\right)\right)$$

$$= \left(\breve{G}_{n,m} + \frac{\breve{g}_{c,nm}}{2}\right)\mathrm{K}_m - G_{n,m}\breve{T}_{n,m} + B_{n,m}\breve{L}_{n,m} \tag{5f}$$

$$\hat{Q}_{m,n} = \gamma\left(-\left(B_{n,m} + \frac{b_{c,nm}}{2} + MG_{n,m}\right)\mathrm{K}_m + B_{n,m}\left(\mathrm{T}_{n,m} - M\mathrm{L}_{n,m}\right)\right.$$

$$\left. + G_{n,m}\left(\mathrm{L}_{n,m} + M\mathrm{T}_{n,m}\right)\right)$$

$$= -\left(\breve{B}_{n,m} + \frac{\breve{b}_{c,nm}}{2}\right)\mathrm{K}_m + B_{n,m}\hat{T}_{n,m} + G_{n,m}\hat{L}_{n,m} \tag{5g}$$

$$P_{G,n}^{min} \le \gamma\left(\hat{P}_{G,n} + M\hat{Q}_{G,n}\right) \le P_{G,n}^{max} \tag{5h}$$

$$Q_{G,n}^{min} \le \gamma\left(\hat{Q}_{G,n} + M\hat{P}_{G,n}\right) \le Q_{G,n}^{max} \tag{5i}$$

$$\left(V^{min}\right)^2 \le \mathrm{K}_n \le (V^{max})^2 \tag{5j}$$

$$\gamma^2\left(\hat{P}_{n,m}+M\hat{Q}_{n,m}\right)^2+\gamma^2\left(\hat{Q}_{n,m}+M\hat{P}_{n,m}\right)^2 \le \left(S_{n,m}^{max}\right)^2 \tag{5k}$$

$$\gamma^2\left(\hat{P}_{m,n}+M\hat{Q}_{m,n}\right)^2+\gamma^2\left(\hat{Q}_{m,n}+M\hat{P}_{m,n}\right)^2 \le \left(S_{n,m}^{max}\right)^2 \tag{5l}$$

In (5a)-(5l), the transformed notations have been marked by adding $(\hat{\cdot})$ and $(\breve{\cdot})$, and they satisfy the following relations:

$$\begin{bmatrix}\breve{g}_{sh,n}\\ \breve{b}_{sh,n}\end{bmatrix} = \gamma\begin{bmatrix}1 & M\\ M & 1\end{bmatrix}\begin{bmatrix}g_{sh,n}\\ b_{sh,n}\end{bmatrix} \tag{6a}$$

$$\begin{bmatrix}\breve{g}_{c,nm}\\ \breve{b}_{c,nm}\end{bmatrix} = \gamma\begin{bmatrix}1 & M\\ M & 1\end{bmatrix}\begin{bmatrix}0\\ b_{c,nm}\end{bmatrix} \tag{6b}$$

$$\begin{bmatrix}\breve{G}_{n,m}\\ \breve{B}_{n,m}\end{bmatrix} = \gamma\begin{bmatrix}1 & M\\ M & 1\end{bmatrix}\begin{bmatrix}G_{n,m}\\ B_{n,m}\end{bmatrix} \tag{6c}$$

$$\begin{bmatrix}\hat{T}_{n,m}\\ \hat{L}_{n,m}\end{bmatrix}=\gamma\begin{bmatrix}1 & -M\\ M & 1\end{bmatrix}\begin{bmatrix}\mathrm{T}_{n,m}\\ \mathrm{L}_{n,m}\end{bmatrix} \tag{6d}$$

$$\begin{bmatrix}\check{T}_{n,m}\\ \check{L}_{n,m}\end{bmatrix}=\gamma\begin{bmatrix}1 & M\\ -M & 1\end{bmatrix}\begin{bmatrix}\mathrm{T}_{n,m}\\ \mathrm{L}_{n,m}\end{bmatrix} \tag{6e}$$

According to the formulation (5)-(6), the relaxed SOCP constraints $\mathrm{T}_{n,m}^2+\mathrm{L}_{n,m}^2\le \mathrm{K}_n\mathrm{K}_m$ can be reformulated based on $\hat{T}_{n,m}$ and $\hat{L}_{n,m}$ (and $\check{T}_{n,m}$ and $\check{L}_{n,m}$) as follows:

$$\left(\hat{T}_{n,m}\right)^2+\left(\hat{L}_{n,m}\right)^2\le\left(\frac{1+M^2}{1-M^2}\right)\mathrm{K}_n\mathrm{K}_m \tag{7a}$$

and

$$\left(\check{T}_{n,m}\right)^2+\left(\check{L}_{n,m}\right)^2\le\left(\frac{1+M^2}{1-M^2}\right)\mathrm{K}_n\mathrm{K}_m \tag{7b}$$

It is obvious that $\left(\frac{1+M^2}{1-M^2}\right)$ is greater than or equal to one. Therefore, the transformed relaxed SOCP constraint provides more space for $\hat{T}_{n,m}$ and $\hat{L}_{n,m}$ (or $\check{T}_{n,m}$ and $\check{L}_{n,m}$) to assign larger values. Consequently, the relaxation error (it will be discussed later) reaches its minimum value for a specific value for *M*.

2.3.2. Model-B: Changing only network parameters

This model attempts to apply the proposed linear transformation on the network data and change the active and reactive demands as well as conductance and susceptance of the branches. The privilege of model-B is that it can be used for estimating the best value for the semi-Lorentz factor for each case according to the network data, and there is no need to find the best semi-Lorentz factor empirically. Therefore, the transformed SOCP- AC OPF can be rewritten as follows.

$$Min_{\forall t}[\mathcal{B}_{Cost}]$$

$$\mathcal{B}_{Cost}=\sum_{n\in\Omega_{bus}}\left(a_n\left(\gamma\left(\hat{P}_{G,n}+M\hat{Q}_{G,n}\right)\right)^2+b_n\left(\gamma\left(\hat{P}_{G,n}+M\hat{Q}_{G,n}\right)\right)+c_n\right) \tag{8a}$$

$$s.t. \qquad \forall n,m\in\Omega_{bus}\ ,\forall(n,m)\in\Omega_{brch}$$

$$\hat{P}_{G,n} - \hat{P}_{D,n} = \breve{g}_{sh,n}\mathrm{K}_n + \sum_{\forall(n,m)\in\Omega_{brch}} \hat{P}_{n,m} \tag{8b}$$

$$\hat{Q}_{G,n} - \hat{Q}_{D,n} = -\breve{b}_{sh,n}\mathrm{K}_n + \sum_{\forall(n,m)\in\Omega_{brch}} \hat{Q}_{n,m} \tag{8c}$$

$$\begin{aligned}\hat{P}_{n,m} = \gamma\Bigg(&\left(\left(G_{n,m} + M\left(B_{n,m} + \frac{b_{c,nm}}{2}\right)\right)K_n - \left(G_{n,m} + MB_{n,m}\right)T_{n,m}\right.\\ &\left. - \left(B_{n,m} - MG_{n,m}\right)L_{n,m}\right)\\ &= \left(\breve{G}_{n,m} + \frac{\breve{g}_{c,nm}}{2}\right)\mathrm{K}_n - \breve{G}_{n,m}\mathrm{T}_{n,m} - \hat{B}_{n,m}\mathrm{L}_{n,m}\end{aligned} \tag{8d}$$

$$\begin{aligned}\hat{Q}_{n,m} = \gamma\Bigg(&-\left(B_{n,m} + \frac{b_{c,nm}}{2} + MG_{n,m}\right)K_n + \left(B_{n,m} + MG_{n,m}\right)T_{n,m}\\ &- \left(G_{n,m} - MB_{n,m}\right)L_{n,m}\Bigg)\\ &= -\left(\breve{B}_{n,m} + \frac{\breve{b}_{c,nm}}{2}\right)\mathrm{K}_n + \breve{B}_{n,m}\mathrm{T}_{n,m} - \hat{G}_{n,m}\mathrm{L}_{n,m}\end{aligned} \tag{8e}$$

$$\begin{aligned}\hat{P}_{m,n} = \gamma\Bigg(&\left(\left(G_{n,m} + M\left(B_{n,m} + \frac{b_{c,nm}}{2}\right)\right)\mathrm{K}_m - \left(G_{n,m} + MB_{n,m}\right)\mathrm{T}_{n,m}\right.\\ &\left. + \left(B_{n,m} - MG_{n,m}\right)\mathrm{L}_{n,m}\right)\\ &= \left(\breve{G}_{n,m} + \frac{\breve{g}_{c,nm}}{2}\right)\mathrm{K}_m - \breve{G}_{n,m}\mathrm{T}_{n,m} + \hat{B}_{n,m}\mathrm{L}_{n,m}\end{aligned} \tag{8f}$$

$$\begin{aligned}\hat{Q}_{m,n} = \gamma\Bigg(&-\left(B_{n,m} + \frac{b_{c,nm}}{2} + MG_{n,m}\right)\mathrm{K}_m + \left(B_{n,m} + MG_{n,m}\right)\mathrm{T}_{n,m}\\ &+ \left(G_{n,m} - MB_{n,m}\right)\mathrm{L}_{n,m}\Bigg)\\ &= -\left(\breve{B}_{n,m} + \frac{\breve{b}_{c,nm}}{2}\right)\mathrm{K}_m + \breve{B}_{n,m}\mathrm{T}_{n,m} + \hat{G}_{n,m}\mathrm{L}_{n,m}\end{aligned} \tag{8g}$$

$$P_{G,n}^{min} \le \gamma\left(\hat{P}_{G,n} + M\hat{Q}_{G,n}\right) \le P_{G,n}^{max} \tag{8h}$$

$$Q_{G,n}^{min} \le \gamma\left(\hat{Q}_{G,n} + M\hat{P}_{G,n}\right) \le Q_{G,n}^{max} \tag{8i}$$

$$\left(V^{min}\right)^2 \le \mathrm{K}_n \le (V^{max})^2 \tag{8j}$$

$$\gamma^2\left(\hat{P}_{n,m}+M\hat{Q}_{n,m}\right)^2+\gamma^2\left(\hat{Q}_{n,m}+M\hat{P}_{n,m}\right)^2 \le \left(S_{n,m}^{max}\right)^2 \tag{8k}$$

$$\gamma^2\left(\hat{P}_{m,n}+M\hat{Q}_{m,n}\right)^2+\gamma^2\left(\hat{Q}_{m,n}+M\hat{P}_{m,n}\right)^2 \le \left(S_{n,m}^{max}\right)^2 \tag{8l}$$

$$\mathrm{T}_{n,m}^2 + \mathrm{L}_{n,m}^2 \le \mathrm{K}_n\mathrm{K}_m \tag{8m}$$

Similarly, in addition to (6a-6c), the mapped network parameters are presented as follows:

$$\begin{bmatrix}\hat{G}_{n,m}\\ \hat{B}_{n,m}\end{bmatrix} = \gamma\begin{bmatrix}1 & -M\\ -M & 1\end{bmatrix}\begin{bmatrix}G_{n,m}\\ B_{n,m}\end{bmatrix} \tag{9}$$

As can be seen, the problem variables (K_n , $\forall n$, $\mathrm{T}_{n,m}$, $\forall (n,m)\in\Omega_{brch}$, and $\mathrm{L}_{n,m}$, $\forall (n,m)\in\Omega_{brch}$) remain unchanged, and semi-Lorentz factor (*M*) plays the main role in changing the network parameters. As already mentioned, the changed parameters are used to estimate the best semi-Lorentz factor for each case separately. This matter will be discussed in more detail in Section 3.3.

3. Experimental results

3.1. The indications for comparison

The error of SOCP relaxation and optimality gap is presented as indications for having a fair comparison with other published works as well as distinguishing what relations are between the optimality gap of transformed SOCP (TSOCP) and SOCP. In more detail, Eq. (10a) is used for finding the error of SOCP relaxation of AC OPF, while the optimality gap between AC OPF and SOCP-AC OPF is calculated by (10b).

$$Error_{SOC} = \sum_{\forall (n,m)\in\Omega_{brch}} \left|\mathrm{K}_n\mathrm{K}_m - \left(\mathrm{T}_{n,m}^2 + \mathrm{L}_{n,m}^2\right)\right| \tag{10a}$$

$$OG = 100 \times \left(\frac{OS_{AC} - OS_{SOCP}}{OS_{AC}}\right) \tag{10b}$$

where, $\boldsymbol{OG}$ is the abbreviation of optimality gap; $\boldsymbol{OS_{AC}}$ and $\boldsymbol{OS_{SOCP}}$ are the optimal solution of non-convex AC OPF and SOCP-AC OPF, respectively.

3.2. Simulation results

The effectiveness of the proposed approach is assessed by implementing it in various case studies in this section. This concept has been simulated in CPLEX software on a laptop with a Core (TM) i7 CPU (2.80 GHz) and 8GB of RAM. Table 1 includes the findings of the optimality gap for all case studies, which are compared to several other methods. These methods are quadratic constraint (QC) and standard SOCP method without transformation. In addition, For the purpose of validating the suggested approach, it is evaluated under three different conditions comprising “typical operating conditions” (TYP), “congested operating conditions” (API), and “small angle difference conditions” (SAD).

When systems are operated under typical conditions, the proposed approach (TSOCP) is ranked as the best one. In more detail, TSOCP witnessed a sharp decline in the optimality gap in case3_lmbd, at 0.1%. The optimality gaps derived from QC and SOCP, on the other hand, are 1.22 and 1.32, respectively. In case5_pjm, the optimality gap for QC, SOCP, and TSOCP is 14.55, 14.55, and 0.086, respectively, suggesting that TSOCP is a better method for decreasing the optimality gap. For case118_ieee, the optimality gap is 0.79, 0.91 and 0 for QC, SOCP, and TSOCP, respectively, meaning that TSOCP is able to find the global optimum precisely. In comparison to other approaches, the proposed solution has the smallest optimality difference for large-scale systems in the normal state, at, 0.97, 1.04, and 0.02 percent, respectively, for QC, SOCP, and TSOCP in case2383wp_k. This comparison reveals that the suggested approach has a good effect on narrowing the optimality gap for small, medium, and large-scale applications, while other measures are exquisitely sensitive to the system size.

Despite the normal condition provided above, all techniques are used to solve the problem when the

systems have a small angle difference. Taking case118_ieee__sad as an example, the proportion of optimality gap for QC, SOCP and TSOCP accounts for 6.84, 8.22 and 0.19 respectively. In this situation, it can be concluded that the suggested method is a very efficient method for solving problems far more efficiently, resulting in outcomes with the smallest optimality gap.

Under congested conditions, the proposed approach is really efficient in terms of reducing the optimality gap. As an example, in case300_ieee__api, QC and SOCP have more optimality gap, accounting for 0.84 and 0.89 percent, respectively, while TSOCP reaches the least optimality gap at 0.043 percent, even comparable to the normal condition. This distinction explicitly indicates that the congested condition does not have a specific impact on the performance of the proposed approach which performs properly.

The proposed methods are also compared with several recently published works shown in Table 1. These are tightened rotated QC (TRQC) ($\psi = 80^{\circ}$) [16], TRQC (ψ^{*}) [16], and improved QC (IQC) [24]. It is clear that the proposed methods are much more precise than other mentioned investigations due to the fact that they have the least optimality gap. As an illustration, the optimality gap for the proposed approach in case118_ieee__api is 0.56%. However, it is 27.11%, 26.38% and 13.61% for TRQC ($\psi = 80^{\circ}$), TRQC (ψ^{*}), and IQC, respectively.

Although transforming OPF equations improves the accuracy of results, it does not increase the complexity of the underlying problem. For more information, the time of running OPF under different situations for different case studies is tabulated in Table 2. From this, it can be seen that the TSOCP takes the time which is similar to SOCP. It takes less time compared to the QC method. It can be seen the TSOCP has more accuracy with less computation time.

Table 1: Optimality gap obtained from different methods

Test Case		AC	QC	SOCP	TSOCP		ETSOCP		TRQC($\psi = 80^{\circ}$) [16]	TRQC(ψ^*) [16]	IQC [24]
		Objective function ($/h)	Gap (%)	Gap (%)	Gap (%)	*M*	Gap (%)	*M*	Gap (%)	Gap (%)	Gap (%)
Case 1	case3_lmbd	5812.64	1.22	1.32	0.1	-0.03	0.1	-0.03	0.84	0.63	0.17
Case 2	case5_pjm	17551.89	14.55	14.55	0.086	-0.36	3.34	-0.41	NA	NA	11.57
Case 3	case39_epri	138415.56	0.55	0.56	0.15	-0.01	0.41	-0.004	NA	NA	NA
Case 4	case89_pegase	107285.67	0.75	0.75	0.17	-0.01	0.56	-0.003	NA	NA	NA
Case 5	case118_ieee	97213.61	0.79	0.91	0	-0.14	0.07	-0.13	0.64	0.62	0.35
Case 6	case2383wp_k	1868170.49	0.97	1.04	0.02	-0.01	0.12	-0.008	NA	NA	NA
Case 7	case3_lmbd__sad	5959.31	1.42	3.75	0.04	-0.08	1.062	-0.06	NA	NA	0.03
Case 8	case14_ieee__sad	2776.79	21.5	21.54	0.31	-0.41	0.31	-0.41	15.82	15.39	NA
Case 9	case30_ieee__sad	8208.52	5.93	9.7	5.05	-0.26	6.29	-0.29	4.56	2.12	NA
Case 10	case89_pegase__sad	107285.67	0.71	0.73	0.1	-0.01	0.43	-0.005	NA	NA	NA
Case 11	case118_ieee__sad	105155.06	6.84	8.22	0.19	-0.45	1.3	-0.48	5.45	5.07	0.67
Case 12	case2383wp_k__sad	1911232.27	1.98	2.93	0.69	-0.43	1.33	-0.35	NA	NA	NA
Case 13	case3_lmbd__api	11235.68	5.63	9.32	0.3	-0.2	2.08	-0.16	4.17	3.93	NA
Case 14	case5_pjm__api	76377.42	4.09	4.09	0.109	-0.27	2.09	-0.18	NA	NA	NA
Case 15	case14_ieee__api	5999.36	5.13	5.13	0.09	-0.12	1.67	-0.16	NA	NA	NA
Case 16	case30_ieee__api	18043.92	5.46	5.46	0	-0.24	2.52	-0.32	NA	NA	NA
Case 17	case39_epri__api	249672.34	1.72	1.74	0.054	-0.04	0.054	-0.04	1.32	1.32	NA
Case 18	case118_ieee__api	242236.8	28.7	28.81	0.56	-0.84	2.78	-0.83	27.11	26.38	13.61
Case 19	case300_ieee__api	684985.5	0.84	0.89	0.043	-0.02	0.572	-0.07	NA	NA	NA

TRQC: tightened rotated QC, ψ^*: best value for rotation, IQC: improved QC.

3.3. An Analysis for determining the best semi-Lorentz factor

If we take a look at Table 1, it can be seen that the semi-Lorentz factor (*M*) has a significant effect on transforming SOCP-AC OPF, and its value is altered with changing the system size and structure. To obtain the best value of *M* for each case, the problem was solved by considering different values of *M* from -0.99 to 0.99, in steps of 0.01. However, this is really time-consuming, not practical and curbs operators from using it in real-time/emergency operations. As a result, three approximations for estimating the best value for *M* for systems in various circumstances are suggested. The proposed estimation equations are obtained via fitting strategies, in which *M* is a function of transformed R/X

and Q/P ratios. It means the best value for the semi-Lorentz factor for each power system category can be estimated by solving the following equations.

- For Typical Operating Conditions (TYP) cases:

$$M = -4\left(\frac{\hat{G}}{\hat{B}}\right)\left(\frac{\hat{Q}}{\hat{P}}\right)^3 = 4\left(\frac{G-MB}{MG-B}\right)\left(\frac{MP-Q}{P-MQ}\right)^3 \quad (11a)$$

- For Congested Operating Conditions (API):

$$M = -1.7\left(\frac{\hat{G}}{\hat{B}}\right)\left(\frac{\hat{Q}}{\hat{P}}\right)^2 = 1.7\left(\frac{G-MB}{MG-B}\right)\left(\frac{MP-Q}{P-MQ}\right)^2 \quad (11b)$$

- For Small Angle Difference Conditions (SAD):

$$M = -\left(\frac{\hat{G}}{\hat{B}}\right)\left(\frac{\hat{Q}}{\hat{P}}\right)^{0.7} = \left(\frac{G-MB}{MG-B}\right)\left(\frac{MP-Q}{P-MQ}\right)^{0.7} \quad (11c)$$

where, G ($\hat{G}$) and B ($\hat{B}$) are the average of network's conductance (transformed conductance in the Model-B) and susceptance (transformed susceptance in the Model-B), respectively. Also, P ($\hat{P}$) and Q ($\hat{Q}$) are the average of active power (transformed active power) and reactive power (transformed reactive power) consumption, respectively.

Column 6 of Table 1 represents the results of the optimality gap for transformed SOCP-OPF via estimated Lorentz factor (ETSOCP) obtained by (11a)-(11c). The results reveal an improvement in the optimality gap of all cases, and the estimated semi-Lorentz factor is merely close to the best semi-Lorentz factor from column 5. To have a better comparison, semi-Lorentz factors for different conditions are depicted in Fig. 3. As can be shown, the proposed estimation method is highly accurate under varying circumstances. In addition, the Pearson correlation coefficient [25] is also used to verify the similarity of estimated semi-Lorentz factors (11a)-(11c) and its best values obtained by empirical analysis (Table 1, column 5). The results show that the Pearson correlation coefficients are 99.46%, 94.7%, and 97.51% for typical operating conditions, congested operating conditions, and

small-angle difference conditions, respectively, which is a great similarity verifying the accuracy of (11a)-(11c).

The relaxation error is also reduced for TSOCP and ETSOCP compared to the normal SOCP. Table 2 represents the percentage of relaxation error reduction of TSOCP and ETSOCP compared to the normal SOCP. Apparently, there are significant improvements in both TSOCP and ETSOCP in terms of relaxation error, which leads to a reduction in the optimality gap (as we can see from Table 1). In other words, there is a direct correlation between the relaxation error and the optimality gap, and the optimality gap changes with respect to the changes in the relaxation error.

In terms of computational time, it is obvious that there is no major difference between typical SOCP, TSOCP, and ETSOCP. In contrast, all these approaches are much faster compared to the QC-OPF.

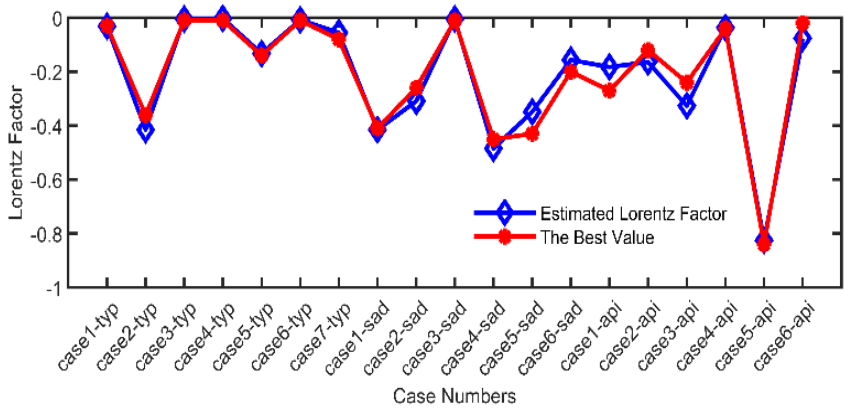

Fig. 3: Comparison of the estimation of semi-Lorentz factor and their best values for different case studies

Table 2: A comparison between transformed and estimated methods

Test Case		*Relaxation Error Reduction (%)		Time (sec.)			
		TSOCP	ETSOCP	QC	SOCP	TSOCP	ETSOCP
Case 1	case3_lmbd	64.32	1.3	1.3	0.6	0.61	0.6
Case 2	case5_pjm	88.64	1.31	1.31	0.61	0.59	0.59
Case 3	case39_epri	99.77	2.01	2.01	1.24	1.25	1.24
Case 4	case89_pegase	91.1	4.38	4.38	3.69	3.21	3.37
Case 5	case118_ieee	100	5.21	5.21	3.47	3.45	3.44
Case 6	case2383wp_k	67.7	51.78	51.78	34.68	34.41	34.59
Case 7	case3_lmbd__sad	86.31	1.29	1.29	0.59	0.6	0.6
Case 8	case14_ieee__sad	99.76	1.39	1.39	0.71	0.69	0.68
Case 9	case30_ieee__sad	94.62	1.84	1.84	1.18	1.19	1.17
Case 10	case89_pegase__sad	74.34	4.26	4.26	3.74	3.51	3.67
Case 11	case118_ieee__sad	99.96	5.19	5.19	3.46	3.47	3.39
Case 12	case2383wp_k__sad	86.24	52.09	52.09	34.9	33.98	33.99
Case 13	case3_lmbd__api	66.66	1.27	1.27	0.59	0.6	0.6
Case 14	case5_pjm__api	99.49	1.32	1.32	0.63	0.61	0.62
Case 15	case14_ieee__api	93.53	1.54	1.54	0.68	0.68	0.68
Case 16	case30_ieee__api	99.31	2.09	2.09	1.15	1.16	1.13
Case 17	case39_epri__api	90.93	2.57	2.57	1.23	1.19	1.21
Case 18	case118_ieee__api	99.85	5.28	5.28	3.41	3.29	3.27
Case 19	case300_ieee__api	23.1	11.92	11.92	7.67	7.59	7.64

$*$ Relaxation Error Reduction for TSOCP $= 100 \times \frac{(Error_{SOC} - Error_{TSOC})}{Error_{SOC}}$, and Relaxation Error Reduction for ETSOCP $= 100 \times \frac{(Error_{SOC} - Error_{ETSOC})}{Error_{SOC}}$

4. Conclusion

Optimal operation of power systems subject to non-linear and non-convex constraints entails an efficient, accurate, and reliable tool. This investigation proposes two different SOCP relaxation mappings of the AC-OPF problem via a new linear transformation (called semi-Lorentz transformation) to enhance the accuracy of SOCP relaxation of AC-OPF. In more detail, two models of transformed SOCP-OPF are presented, including the transformation of network parameters and variables of the problem. The proposed transformation is linear and does not affect the convexity of the SOCP-OPF problem. An empirical analysis is done to obtain a good value for the semi-Lorentz factor (M). Then three equations (obtained by fitting strategies) are developed to suggest a good estimation for the best value for M. Compared to the typical SOCP and QC relaxation of AC-OPF, the results reveal a significant improvement in both optimality gap and relaxation error. Our ongoing work is to develop a dynamic approximation for linear-OPF to enhance the result accuracy as much as possible. For future work, we will also consider the proposed linear transformation for mapping the quadratic constrained OPF (QC-OPF).

5. References

[1] D. Bienstock and A. Verma, "Strong NP-hardness of AC power flows feasibility," *Oper. Res. Lett.*, vol. 47, no. 6, pp. 494–501, Nov. 2019, doi: 10.1016/j.orl.2019.08.009.

[2] M. Ghasemi, S. Ghavidel, E. Akbari, and A. A. Vahed, "Solving non-linear, non-smooth and non-convex optimal power flow problems using chaotic invasive weed optimization algorithms based on chaos," *Energy*, vol. 73, pp. 340–353, Aug. 2014, doi: 10.1016/j.energy.2014.06.026.

[3] M. Ghasemi, S. Ghavidel, M. M. Ghanbarian, M. Gharibzadeh, and A. Azizi Vahed, "Multi-objective optimal power flow considering the cost, emission, voltage deviation and power losses using multi-objective modified imperialist competitive algorithm," *Energy*, vol. 78, pp. 276–289, Dec. 2014, doi: 10.1016/j.energy.2014.10.007.

[4] A. Alhejji, M. Ebeed Hussein, S. Kamel, and S. Alyami, "Optimal Power Flow Solution with an Embedded Center-Node Unified Power Flow Controller Using an Adaptive Grasshopper Optimization Algorithm," *IEEE Access*, vol. 8, pp. 119020–119037, 2020, doi: 10.1109/ACCESS.2020.2993762.

[5] W. A. Bukhsh, A. Grothey, K. I. M. McKinnon, and P. A. Trodden, "Local solutions of the optimal power flow problem," *IEEE Trans. Power Syst.*, vol. 28, no. 4, pp. 4780–4788, 2013, doi: 10.1109/TPWRS.2013.2274577.

[6] M. R. Narimani, D. K. Molzahn, D. Wu, and M. L. Crow, "Empirical Investigation of Non-Convexities in Optimal Power Flow Problems," in *Proceedings of the American Control Conference*, 2018, vol. 2018–June, pp. 3847–3854, doi: 10.23919/ACC.2018.8431760.

[7] J. Lavaei and S. H. Low, "Zero duality gap in optimal power flow problem," *IEEE Trans. Power Syst.*, vol. 27, no. 1, pp. 92–107, Feb. 2012, doi: 10.1109/TPWRS.2011.2160974.

[8] X. Bai, H. Wei, K. Fujisawa, and Y. Wang, "Semidefinite programming for optimal power

flow problems," *Int. J. Electr. Power Energy Syst.*, vol. 30, no. 6–7, pp. 383–392, Jul. 2008, doi: 10.1016/j.ijepes.2007.12.003.

[9] B. C. Lesieutre, D. K. Molzahn, A. R. Borden, and C. L. DeMarco, "Examining the limits of the application of semidefinite programming to power flow problems," in *2011 49th Annual Allerton Conference on Communication, Control, and Computing, Allerton 2011*, 2011, pp. 1492–1499, doi: 10.1109/Allerton.2011.6120344.

[10] J. Lavaei, D. Tse, and B. Zhang, "Geometry of power flows and optimization in distribution networks," *IEEE Trans. Power Syst.*, vol. 29, no. 2, pp. 572–583, Mar. 2014, doi: 10.1109/TPWRS.2013.2282086.

[11] S. H. Low, "Convex relaxation of optimal power flow - Part i: Formulations and equivalence," *IEEE Trans. Control Netw. Syst.*, vol. 1, no. 1, pp. 15–27, Mar. 2014, doi: 10.1109/TCNS.2014.2309732.

[12] S. H. Low, "Convex relaxation of optimal power flow-part II: Exactness," *IEEE Trans. Control Netw. Syst.*, vol. 1, no. 2, pp. 177–189, 2014, doi: 10.1109/TCNS.2014.2323634.

[13] B. Kocuk, S. S. Dey, and X. A. Sun, "Inexactness of SDP relaxation and valid inequalities for optimal power flow," *IEEE Trans. Power Syst.*, vol. 31, no. 1, pp. 642–651, Jan. 2016, doi: 10.1109/TPWRS.2015.2402640.

[14] C. Chen, A. Atamtürk, and S. S. Oren, "A spatial branch-and-cut method for non-convex QCQP with bounded complex variables," *Math. Program.*, vol. 165, no. 2, pp. 549–577, Oct. 2017, doi: 10.1007/s10107-016-1095-2.

[15] C. Chen, A. Atamturk, and S. S. Oren, "Bound tightening for the alternating current optimal power flow problem," *IEEE Trans. Power Syst.*, vol. 31, no. 5, pp. 3729–3736, Sep. 2016, doi: 10.1109/TPWRS.2015.2497160.

[16] M. R. Narimani, D. K. Molzahn, and M. L. Crow, “Tightening QC Relaxations of AC Optimal Power Flow Problems via Complex per Unit Normalization,” *IEEE Trans. Power Syst.*, vol. 36, no. 1, pp. 281–291, Jan. 2021, doi: 10.1109/TPWRS.2020.3004289.

[17] Z. Miao, L. Fan, H. G. Aghamolki, and B. Zeng, “Least squares estimation based SDP cuts for SOCP relaxation of AC OPF,” *IEEE Trans. Automat. Contr.*, vol. 63, no. 1, pp. 241–248, Jan. 2018, doi: 10.1109/TAC.2017.2719607.

[18] C. Coffrin, H. L. Hijazi, and P. Van Hentenryck, “The QC Relaxation: A Theoretical and Computational Study on Optimal Power Flow,” *IEEE Trans. Power Syst.*, vol. 31, no. 4, pp. 3008–3018, Jul. 2016, doi: 10.1109/TPWRS.2015.2463111.

[19] Z. Yuan and M. Paolone, “Properties of convex optimal power flow model based on power loss relaxation,” *Electr. Power Syst. Res.*, vol. 186, p. 106414, Sep. 2020, doi: 10.1016/j.epsr.2020.106414.

[20] S. Y. Abdelouadoud, R. Girard, F. P. Neirac, and T. Guiot, “Optimal power flow of a distribution system based on increasingly tight cutting planes added to a second order cone relaxation,” *Int. J. Electr. Power Energy Syst.*, vol. 69, pp. 9–17, Jul. 2015, doi: 10.1016/j.ijepes.2014.12.084.

[21] S. Lang, *Linear Algebra*. New York, NY: Springer New York, 1987.

[22] R. A. Jabr, “Radial distribution load flow using conic programming,” *IEEE Trans. Power Syst.*, vol. 21, no. 3, pp. 1458–1459, Aug. 2006, doi: 10.1109/TPWRS.2006.879234.

[23] M. Bynum, A. Castillo, J. P. Watson, and C. D. Laird, “Tightening McCormick relaxations toward global solution of the ACOPF problem,” *IEEE Trans. Power Syst.*, vol. 34, no. 1, pp. 814–817, Jan. 2019, doi: 10.1109/TPWRS.2018.2877099.

[24] M. R. Narimani, D. K. Molzahn, and M. L. Crow, “Improving QC relaxations of OPF

problems via voltage magnitude difference constraints and envelopes for trilinear monomials," *arXiv*, 2018.

[25] J. Benesty, J. Chen, Y. Huang, and I. Cohen, "Pearson correlation coefficient," in *Springer Topics in Signal Processing*, vol. 2, Springer Science and Business Media B.V., 2009, pp. 1–4.